

The energetics and mechanism of fluxionality of 2,2':6',2''-terpyridine derivatives when acting as bidentate ligands in transition-metal complexes. A detailed dynamic NMR study

Andrew Gelling, Keith G. Orrell,* Anthony G. Osborne and Vladimir Šik

Department of Chemistry, The University, Exeter, UK EX4 4QD

Syntheses are reported for the following transition metal complexes of derivatives of 2,2':6',2''-terpyridine, [ReBr(CO)₃L] (L = mcpt, mcpmt, mmtt or bmtt), [PtIME₃(mcpt)], [Pd(C₆F₅)₂(mcpt)] and [Pt(C₆F₅)₂(mcpt)] where mcpt = 4-methyl-4'-(4-chlorophenyl)-2,2':6',2''-terpyridine, mcpmt = 4-methyl-4'-(4-chlorophenyl)-4''-methyl-2,2':6',2''-terpyridine, mmtt = 4-methyl-4'-methylthio-2,2':6',2''-terpyridine and bmtt = 4-*tert*-butyl-4'-methylthio-2,2':6',2''-terpyridine. In organic solvents (CD₂Cl₂, CDCl₂-CDCl₂) they exist as bidentate chelate complexes which undergo double 1,4-metallotropic shifts ('tick-tock' twists). These shifts have been monitored by variable temperature one- and two-dimensional NMR methods and activation energy data obtained. These energy data are very metal-dependent, magnitudes of Δ*G*[‡] (298.15 K) being in the range 66–101 kJ mol⁻¹ and showing the trend Pt^{II} ≫ Pd^{II} ≈ Re^I > Pt^{IV}. The nature of the ligand does not greatly influence the ligand fluxionality but does affect the relative populations of the pairs of metal complexes found in solution (when L = mcpt, mmtt and bmtt). Above-ambient temperature 2-D-exchange spectroscopy (EXSY) NMR experiments provide firm evidence for the fluxions occurring by an associative mechanism, involving five-co-ordinate intermediates for palladium(II) and platinum(II) complexes, and seven-co-ordinate intermediates for platinum(IV) and, by analogy, rhenium(I) complexes.

Whilst a planar N₃ heterocyclic compound such as 2,2':6',2''-terpyridine (terpy) usually behaves as a terdentate ligand towards many metals, it will act as a bidentate chelate in certain types of kinetically inert complexes, for example, those involving metal moieties of facial geometry such as *fac*-PtXMe₃ and *fac*-ReX(CO)₃ (where X is halogen), and *cis*-square planar metal moieties such as *cis*-ML₂ where M = Pd^{II} or Pt^{II} and L = C₆F₅, *etc.* In such circumstances, however, the N₃ ligand is fluxional and switches its metal co-ordination between different adjacent pairs of its three nitrogen donors. This process has been extensively studied by NMR spectroscopy by ourselves¹⁻⁵ and by others,⁶⁻⁸ and the factors governing the rates and energies of the fluxion assessed.

In our earlier work¹⁻⁵ we proposed an associative mechanism for the fluxional shift whereby the metal moiety twists through an angle equal to the N–M–N angle of the metal centre involving a seven- or five-co-ordinate metal intermediate. Such a 'tick-tock' twist mechanism accounts for the observation that the chemical environments of the ligands attached to the metal *trans* to the M–N bonds are invariably exchanged during this process. However, this mechanism has been questioned⁹ in the case of the square-planar complexes *cis*-[M(C₆F₅)₂(terpy)] (M = Pd^{II} or Pt^{II}), and an alternative dissociative process, based on a T-shaped 14-electron, three-co-ordinate intermediate, proposed.

In order to resolve this matter conclusively it became evident to us that metal complexes of unsymmetrical derivatives of terpy, in which the fluxion caused an interchange between chemically different co-ordination complexes, needed to be studied.

Accordingly, we have synthesised the unsymmetrical ligands 4-methyl-4'-(4-chlorophenyl)-2,2':6',2''-terpyridine (mcpt), 4-methyl-4'-methylthio-2,2':6',2''-terpyridine (mmtt) and 4-*tert*-butyl-4'-methylthio-2,2':6',2''-terpyridine (bmtt), in addition to the symmetrical ligand 4-methyl-4'-(4-chlorophenyl)-4''-methyl-2,2':6',2''-terpyridine (mcpmt). These compounds were then co-ordinated with Re^I, Pt^{IV}, Pd^{II} and Pt^{II} to give the complexes [ReBr(CO)₃L] (L = mcpt, mcpmt, mmtt or bmtt), [PtIME₃(mcpt)], [Pd(C₆F₅)₂(mcpt)] and [Pt(C₆F₅)₂(mcpt)].

We now report our dynamic NMR findings on these complexes. A preliminary report on some of this work has been published.¹⁰

Experimental

Materials

The compounds [ReBr(CO)₃],¹¹ [PtIME₃]₄,¹² [Pt(C₆F₅)₂(1,4-dioxane)₂],¹³ [Pd(C₆F₅)₂(C₄H₉S)₂],¹⁴ 2-cyano-4-methylpyridine,¹⁵ 2-acetyl-4-methylpyridine,¹⁶ 4-*tert*-butylpyridine *N*-oxide¹⁷ and *N*-[2-oxo-2-(2'-pyridyl)ethyl]pyridinium iodide¹⁸ were prepared according to literature methods.

Synthesis of terpyridines

The compound *N*-{2-oxo-2-[2'-(4'-methylpyridyl)]ethyl}pyridinium iodide was prepared from 2-acetyl-4-methylpyridine according to a literature method¹⁸ but using a reaction temperature of 70 °C, to yield the desired product as an orange crystalline material.

1-{3-oxo-3-[2-(4-methylpyridyl)]propen-1-yl}-4-chlorobenzene. To a stirred solution of 2-acetyl-4-methylpyridine (1.0 g, 7.4 mmol) in ethanol (20 cm³), 4-chlorobenzaldehyde (1.6 g, 11.3 mmol) was added, followed by aqueous sodium hydroxide (3 cm³, 1 M) and water (4 cm³). The resulting mixture was stirred for 4 h, after which time the yellow precipitate which had formed was collected by filtration, washed with ethanol (2 × 50 cm³) and dried under vacuum to give a pale yellow solid. Yield 0.78 g (28%), *m/z* (EI) 257 (*M*⁺), δ_H(300 MHz, CDCl₃) 2.45 (3 H, s, Me), 7.30 (1 H, d, *J* 4.9, H⁵), 7.38 (2 H, d, *J* ≈ 8.5, H_m), 7.64 (2 H, d, *J* ≈ 8.5 H_o), 7.85 (1 H, d, *J* 16.1, CH), 8.00 (1 H, s, H³), 8.24 (1 H, d, *J* 16.1, CH), 8.58 (1 H, d, *J* 4.9 Hz, H⁶).

2-Cyano-4-*tert*-butylpyridine was prepared from 4-*tert*-butylpyridine *N*-oxide by following a literature method¹⁵ to yield the desired product as a pale yellow oil in 95% yield. δ_H(300 MHz, CDCl₃) 1.27 (9 H, s, Bu^t), 7.45 (1 H, dd, *J* 4.9, 1.5, H⁵), 7.63 (1 H, d, *J* 1.5, H³), 8.52 (1 H, d, *J* 4.9 Hz, H⁶).

Table 1 Analytical data for the complexes *fac*-[ReBr(CO)₃L] (L = mcpt, mcpmt, mmtt or bmtt) and [M(mcpt)] [M = PtMe₃, Pt(C₆F₅)₂ or Pd(C₆F₅)₂]

Complex	Yield ^a (%)	ν_{CO} ^b /cm ⁻¹	Analysis ^c (%)		
			C	H	N
[ReBr(CO) ₃ (mcpt)]	75	2021s 1918m 1892m	42.2 (42.4)	1.9 (2.3)	5.8 (5.9)
[PtMe ₃ (mcpt)]	69	—	42.2 (41.4)	3.8 (3.4)	5.2 (5.8)
[Pt(C ₆ F ₅) ₂ (mcpt)]	37	—	46.1 (46.0)	2.2 (1.8)	4.5 (4.7)
[Pd(C ₆ F ₅) ₂ (mcpt)]	26	—	51.8 (51.1)	2.5 (2.0)	5.3 (5.3)
[ReBr(CO) ₃ (mcpmt)]	41	2027s 1915m 1893m	42.9 (43.2)	2.0 (2.5)	5.0 (5.8)
[ReBr(CO) ₃ (mmtt)]	64	2023s 1921m 1896m	35.9 (37.3)	2.1 (2.3)	6.1 (6.5)
[ReBr(CO) ₃ (bmtt)] ^d	26	2023s 1922m 1898m			

^a Yield quoted relative to metal containing reactant. ^b Recorded in benzene solution; s = strong, m = medium. ^c Calculated values in parentheses. ^d Satisfactory analysis could not be obtained.

2-Acetyl-4-*tert*-butylpyridine. To a stirred solution of 2-cyano-4-*tert*-butylpyridine (4.0 g, 22.2 mmol) in benzene (400 cm³), cooled in an ice-water bath, methylmagnesium iodide (8 cm³, 3 M in diethyl ether) was added. After stirring at low temperature for 1 h the solution was allowed to attain room temperature and stirred for 14 h, after which time water (100 cm³) was carefully added, followed by sulfuric acid (100 cm³, 2 M) and the resulting mixture stirred for a further 14 h. The aqueous layer was separated, made neutral by the addition of sodium hydroxide, and then extracted with dichloromethane (3 × 120 cm³). The extract was dried over MgSO₄ followed by removal of solvent under reduced pressure to yield the desired product as a dark yellow oil (4.1 g) in 93% yield. δ_{H} (300 MHz, CDCl₃) 1.35 (9 H, s, Bu^t), 2.73 (3 H, s, Me), 7.45 (1 H, dd, *J* 4.9, 1.5, H⁵), 8.05 (1 H, d, *J* 1.5, H³), 8.57 (1 H, d, *J* 4.9 Hz, H⁶).

4-Methyl-4'-(4-chlorophenyl)-2,2':6',2''-terpyridine (mcpt) and 4-methyl-4'-(4-chlorophenyl)-4''-methyl-2,2':6',2''-terpyridine (mcpmt) were prepared from the reaction of 1-{3-oxo-3-[2-(4-methylpyridyl)]propen-1-yl}-4-chlorobenzene with *N*-[2-oxo-2-(2'-pyridyl)ethyl]pyridinium iodide or *N*-[2-oxo-2-[2'-(4'-methylpyridyl)ethyl]pyridinium iodide respectively according to the original method of Krohnke¹⁹ and latterly of Constable and Cargill-Thompson.²⁰ The preparation of 4-methyl-4'-(4-chlorophenyl)-4''-methyl-2,2':6',2''-terpyridine is described below in more detail.

4-Methyl-4'-(4-chlorophenyl)-4''-methyl-2,2':6',2''-terpyridine (mcpmt). To a stirred solution of 1-{3-oxo-3-[2-(4-methylpyridyl)]propen-1-yl}-4-chlorobenzene (2.26 g, 8.8 mmol) in ethanol (60 cm³), *N*-[2-oxo-2-[2'-(4'-methylpyridyl)ethyl]pyridinium iodide (2.99 g, 8.8 mmol) and ammonium acetate (18 g, large excess) were added and the resulting solution heated under reflux for 48 h, after which time a pale yellow precipitate had formed. After cooling the mixture to room temperature the precipitate was collected by filtration and washed with cold ethanol (2 × 50 cm³) to give the product as a cream coloured solid (0.75 g) in 23% yield.

4-Methyl-4'-methylthio-2,2':6',2''-terpyridine (mmtt) and 4-*tert*-butyl-4'-methylthio-2,2':6',2''-terpyridine (bmtt) were prepared from the reaction of 2-acetylpyridine with 2-acetyl-4-methylpyridine or 2-acetyl-4-*tert*-butylpyridine respectively according to the original method of Potts *et al.*²¹ The preparation of 4-*tert*-butyl-4'-methylthio-2,2':6',2''-terpyridine is described below in more detail.

4-*tert*-Butyl-4'-methylthio-2,2':6',2''-terpyridine (bmtt). To potassium *tert*-butoxide (3.8 g, 33.9 mmol) in tetrahydrofuran (120 cm³), 2-acetylpyridine (2.05 g, 16.9 mmol) was added

dropwise over 15 min followed by carbon disulfide (1.3 g, 17.1 mmol) and iodomethane (4.8 g, 33.8 mmol), both added dropwise. The resulting mixture was stirred for 6 h, after which time a solution of 2-acetyl-4-*tert*-butylpyridine (3.0 g, 16.9 mmol) and potassium *tert*-butoxide (3.8 g, 33.9 mmol) in tetrahydrofuran (60 cm³) was added and the resulting deep red solution stirred for 14 h. Glacial acetic acid (21 cm³) and ammonium acetate (13.0 g) were added and after 15 min the solvent was removed by distillation over 4 h, to leave a black tar. The tar was washed with ethanol (100 cm³) and then extracted with hexane (2 × 150 cm³). Removal of the solvent under reduced pressure produced the desired product as an orange oil (3.4 g) in 60% yield.

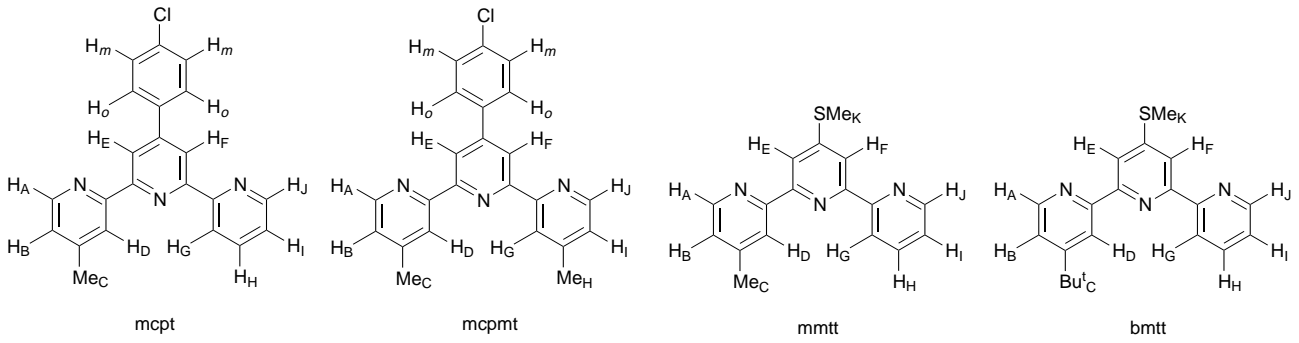
Synthesis of complexes

All preparations were carried out using standard Schlenk techniques²² under purified nitrogen using freshly distilled and degassed solvents. The complexes [ReBr(CO)₃L] (L = mcpt, mcpmt, mmtt or bmtt), [PtMe₃(mcpt)], [M(C₆F₅)₂(mcpt)] (M = Pd or Pt) were all prepared using methods analogous to those reported^{2,3,5} for the preparation of the corresponding complexes of 2,2':6',2''-terpyridine, except that, for the palladium complex, [Pd(C₆F₅)₂(C₄H₈S)₂] was the metal precursor.

Synthetic and analytical data for all the complexes are given in Table 1.

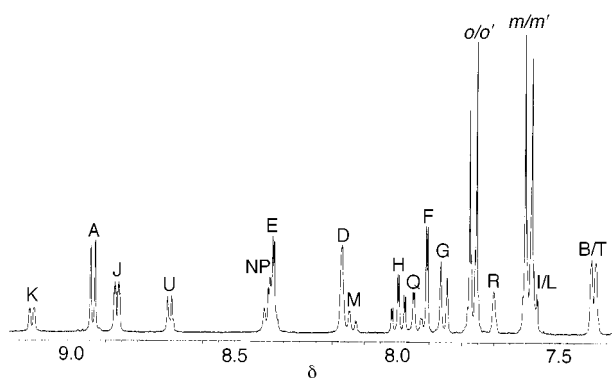
Physical methods

Hydrogen-1 NMR spectra were recorded on Bruker AC-300 or DRX-400 spectrometers operating at 300 or 400 MHz respectively. The DRX-400 spectrometer was also used to record ¹⁹F spectra (376 MHz), ¹³C spectra (101 MHz) and ¹⁹⁵Pt spectra (86 MHz). All spectra were recorded as CDCl₃, CD₂Cl₂ or (CDCl₂)₂ solutions, ¹H and ¹³C NMR chemical shifts are quoted relative to Me₄Si ($\delta = 0$), ¹⁹F shifts relative to C₆F₆ ($\delta = 0$) and ¹⁹⁵Pt shifts relative to the absolute frequency Ξ (¹⁹⁵Pt = 21.4 MHz). Variable-temperature NMR spectra were recorded on the DRX-400 spectrometer using the Bruker B-VT-2000 variable-temperature unit to control the probe temperature, calibration being periodically checked against a Comark digital thermometer. Sample temperatures are considered accurate to ± 1 °C. Two-dimensional exchange (EXSY) spectra and homonuclear correlated (COSY) spectra were obtained using the standard Bruker programs NOESYPH.AU and COSY.AU respectively. Mixing times in the EXSY experiments were chosen in the range 0.5–0.8 s according to the nature of the complex and the temperature of the measurement. Rate data were based on band-shape analysis of ¹H spectra using the

Table 2 Hydrogen-1 NMR data^a for the ligands mcpt, mcpmt, mmtt and bmtt


Ligand	δ												
	H _A	H _B	H _C	H _D	H _E	H _F	H _G	H _H	H _I	H _J	H _K	H _o	H _m
mcpt	8.57	7.17	2.50	8.46	8.67	8.67	8.66	7.88	7.34	8.71	—	7.82 ^b	7.46
mcpmt	8.57	7.17	2.51	8.46	8.66	8.66	8.46	2.51	7.17	8.57	—	7.82 ^c	7.46
mmtt	8.54	7.15	2.48	8.41	8.30	8.30	8.61	7.86	7.33	8.69	2.65	—	—
bmtt	8.61	7.31	1.41	8.60	8.32	8.30	8.58	7.84	7.30	8.68	2.63	—	—

^a Chemical shifts, recorded in CDCl₃ at 303 K relative to internal SiMe₄ ($\delta = 0$). ^b $J_{o,m}$ 8.68 Hz. ^c $J_{o,m}$ 8.34 Hz.

**Fig. 1** 400 MHz ¹H NMR spectrum (aromatic region) of [ReBr(CO)₃(mcpt)] in (CDCl₂)₂ at 293 K. See Table 3 for labelling

authors' version of the standard DNMR3 program,²³ or from 2-D-EXSY spectra using volume integration data in the authors' D2DNMR program.²⁴ Activation parameters based on experimental rate data were calculated using the THERMO program.²⁵

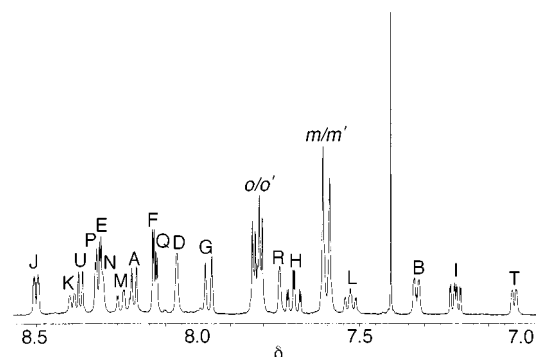
Infrared spectra were recorded on a Perkin-Elmer 881 spectrometer calibrated from the signal of polystyrene at 1602 cm⁻¹. The electron impact mass spectrum was obtained on a Kratos Profile spectrometer. Elemental analyses were performed by Butterworth Laboratories, Teddington, Middlesex, London.

Results

Ambient-temperature NMR studies

Room-temperature ¹H NMR data for the four ligands are given in Table 2 and are consistent with expectations. The ligands are depicted in this Table with all rings coplanar and with the peripheral pyridyl rings adopting a conformation whereby their N heteroatoms are *trans* with respect to the central pyridyl N atom. Such a *trans:trans* structure occurs exclusively in the solid state for terpy itself.²⁶

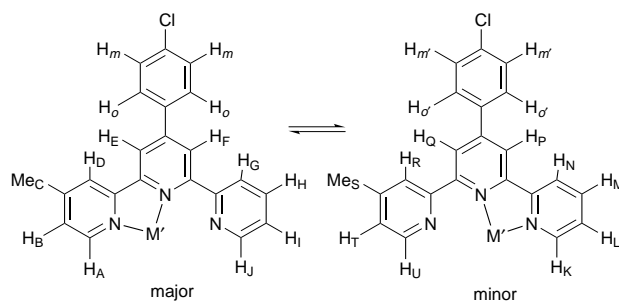
Metal co-ordination causes all the ligands to adopt *cis:cis* configurations. Co-ordination of mcpt gives rise to a pair of complexes which, in solution, interchange as a result of the double 1,4-metallotropic shift. Full ¹H NMR chemical shift data for the four mcpt complexes are given in Table 3. Assignments were based on COSY experiments and previous experience of the expected metal co-ordination shifts of the ring

**Fig. 2** 400 MHz ¹H NMR spectrum (aromatic region) of [Pt(C₆F₅)₂(mcpt)] in (CDCl₂)₂ at 313 K. See Table 3 for labelling. Singlet at δ 7.4 is due to benzene

hydrogens. The abundance ratios of the pairs of complexes in CD₂Cl₂ or (CDCl₂)₂ solutions were approximately 2:1 in all cases. The major solution species were attributed to those with co-ordination to the 4-methylpyridyl ring, because of the large high-frequency co-ordination shifts of the ring hydrogen H_A, and the slightly smaller shifts of H_B, and Me_C in the rhenium(i) and platinum(iv) complexes. The hydrogens on the un-co-ordinated pyridyl ring experience rather smaller positive shifts. H_G and H_D are shifted to low frequency as a result of the change in ligand conformation from *trans:trans* to *cis:cis*. This effect has been noted previously in related bispyrazolopyridine ligands when complexed to Re¹.²⁷

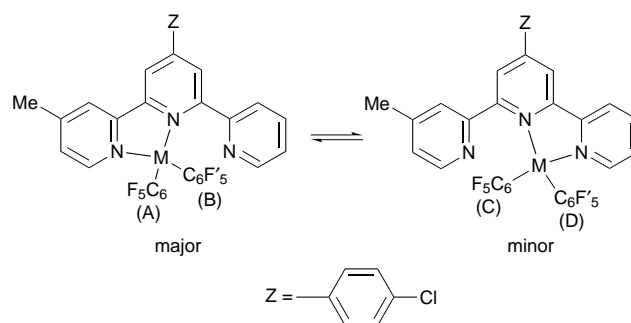
The aromatic region of the ¹H NMR spectrum of [ReBr(CO)₃(mcpt)] in (CDCl₂)₂ at 293 K is shown in Fig. 1, with signals labelled according to Table 3. The separations of the high frequency signals H_A–H_U and H_J–H_K represent *internal* co-ordination shifts and are of opposite sign, in accordance with the structures shown in Table 3. The signals of the 4-chlorophenyl ring show fine structure typical of an AA'BB' spin system.

The ¹H NMR spectrum of [Pt(C₆F₅)₂(mcpt)] in (CDCl₂)₂ at 313 K is depicted in Fig. 2. This displays a quite different distribution of shifts for the pyridyl hydrogens compared to the rhenium(i) complex. In general the shifts are to lower frequencies of the corresponding signals in the rhenium(i) complex, and notably the relative shifts of H_A and H_U, and of H_J and H_K are reversed relative to those in the rhenium(i) complex. This has been noted before in the corresponding terpy complex³ and is a result of H_A and H_K being in the shielding zone of the

Table 3 Hydrogen-1 NMR data^a for the complexes [M'(mcpt)]

M'	Isomer	δ												
ReBr(CO) ₃ ^b	Major	8.92 (A)	7.39 (B)	2.63 (C)	8.24 (D)	8.45 (E)	7.93 (F)	7.85 (G)	7.97 (H)	7.55 (I)	8.83 (J)	7.81 (o)	7.59 (m)	
	Minor	8.67 (U)	7.37 (T)	2.50 (S)	7.71 (R)	7.98 (Q)	8.41 (P)	8.44 (N)	8.16 (M)	7.58 (L)	9.11 (K)	7.80 (o')	7.58 (m')	
PtIme ₃ ^c	Major	8.89 (A)	7.50 (B)	2.61 (C)	8.11 (D)	8.33 (E)	8.11 (F)	8.58 (G)	7.91 (H)	8.15 (I)	8.76 (J)	7.80 (o)	7.57 (m)	
	Minor	8.61 (U)	7.29 (T)	2.51 (S)	8.47 (R)	8.15 (Q)	8.34 (P)	8.54 (N)	8.15 (M)	7.69 (L)	9.09 (K)	7.80 (o')	7.57 (m')	
Pt(C ₆ F ₅) ₂ ^d	Major	8.20 (A)	7.32 (B)	2.54 (C)	8.06 (D)	8.30 (E)	8.14 (F)	7.97 (G)	7.70 (H)	7.20 (I)	8.50 (J)	7.82 (o)	7.60 (m)	
	Minor	8.36 (U)	7.02 (T)	2.41 (S)	7.75 (R)	8.13 (Q)	8.32 (P)	8.30 (N)	8.23 (M)	7.53 (L)	8.39 (K)	7.81 (o')	7.60 (m')	
Pd(C ₆ F ₅) ₂ ^e	Major	7.86 (A)	7.35 (B)	2.63 (C)	8.06 (D)	8.31 (E)	8.14 (F)	7.91 (G)	7.73 (H)	7.22 (I)	8.50 (J)	7.82 (o)	7.61 (m)	
	Minor	8.36 (U)	7.03 (T)	2.44 (S)	7.69 (R)	8.10 (Q)	8.30 (P)	8.04 (N)	8.13 (M)	7.50 (L)	8.29 (K)	7.81 (o')	7.61 (m')	

^a Chemical shifts relative to internal SiMe₄, $\delta = 0$. ^b In CD₂Cl₂ at 273 K. ^c In (CDCl₂)₂ at 263 K. ^d In (CDCl₂)₂ at 313 K. ^e In (CDCl₂)₂ at 303 K.

Table 4 Fluorine-19 NMR data^a for the complexes [M(C₆F₅)₂(mcpt)] (M = Pd^{II} or Pt^{II})

Complex	<i>o</i> -F		<i>m</i> -F		<i>p</i> -F	
	Major	Minor	Major	Minor	Major	Minor
M = Pd ^b	48.99 (A)	48.32 (C) ^c	1.47 (A)	0.01 (C) ^c	4.04 (A)	1.88 (C)
	48.23 (B) ^c	49.27 (D)	0.01 (B) ^c	1.53 (D)	1.86 (B)	4.19 (D)
M = Pt ^d	46.27 (A)	45.58 (C) ^c	-0.06 (A)	-1.34 (C)	2.31 (A)	0.21 (C)
	45.58 (B) ^c	46.55 (D)	-1.38 (B)	0.06 (D)	0.095 (B)	2.47 (D)

^a Chemical shifts relative to C₆F₆ ($\delta = 0$). ^b In (CDCl₂)₂ at 313 K. ^c Overlapping signals. ^d In (CDCl₂)₂ at 413 K.

adjacent pentafluorophenyl ring which resides preferentially in a near-orthogonal position with respect to the pyridyl rings.

Fluorine-19 NMR chemical shift and scalar coupling constant data for the pentafluorophenyl rings are given in Tables 4 and 5. The pairs of non-equivalent C₆F₅ rings are labelled A and B (major solution complex) and C and D (minor solution complex). The chemical shift assignments of these rings are given in Table 4. They are based on the assumption that the fluorines of C₆F₅ rings adjacent to the co-ordinated pyridyl ring (*viz.* rings A and D) will experience the ring current of this pyridyl ring and their ¹⁹F signals will be deshielded with respect to the corresponding fluorines of the other C₆F₅ rings (rings B and C). The latter will experience an overall shielding effect of the pendant pyridyl ring because the latter prefers to adopt a near-orthogonal orientation with respect to the other pyridyl rings (see later).

Additional ¹H, ¹³C and ¹⁹⁵Pt NMR data for the complexes [ReBr(CO)₃(mcpt)] and [PtIme₃(mcpt)] are listed in Table 6. Signal assignments of the pairs of non-equivalent equatorial ligands (*viz.* carbonyls or methyls) were based on previous

studies.^{2,3} The more deshielded signal in both cases was due to the equatorial group adjacent to the co-ordinated pyridyl ring.

Room-temperature ¹H NMR data for the complexes [ReBr(CO)₃L] (L = mmtt or bmtt) are listed in Table 7, and the corresponding data for the symmetrical ligand complex [ReBr(CO)₃(mcpt)] are given in Table 8. All assignments in Tables 7 and 8 are considered to be firm.

Low-temperature NMR studies

The rotational properties of the pendant pyridyl rings were investigated by low-temperature NMR studies of the complexes [ReBr(CO)₃(mcpt)] and [PtIme₃(mcpt)] in CD₂Cl₂ solutions. A quantitative study was performed on [ReBr(CO)₃(mcpt)]. Cooling this complex to *ca.* 173 K caused changes in most of the signals, those due to H_D, H_F and Me_C of the major solution complex and H_K, H_Q and H_R of the minor complex being most clearly observed (see Table 3 for labelling). In all these cases the signals broadened initially on cooling and eventually split into slightly unequal intensity pairs at the lowest temperatures. An

Table 5 Fluorine-19 NMR spin–spin coupling constants (Hz) for the complexes $[M(C_6F_5)_2(mcpt)]$ ($M = Pd^{II}$ or Pt^{II})

Complex	Major isomer				Minor isomer			
	Ring A		Ring B		Ring C		Ring D	
	$J_{o,m}$	$J_{m,p}$	$J_{o,m}$	$J_{m,p}$	$J_{o,m}$	$J_{m,p}$	$J_{o,m}$	$J_{m,p}$
M = Pd	30.0	20.1	29.4	20.2	35.2	20.1	30.4	20.2
M = Pt	31.7 ^a	19.2	— ^{b,c}	19.1	— ^{b,c}	19.3	31.9 ^d	19.2

^a $^3J(^{195}Pt-^{19}F) = 432$ Hz. ^b Overlapping signals, spin–spin couplings not measurable. ^c $^3J(^{195}Pt-^{19}F) \approx 455$ Hz. ^d $^3J(^{195}Pt-^{19}F) = 440$ Hz.

Table 6 Additional 1H , ^{13}C and ^{195}Pt NMR data for the complexes $[M(mcpt)]$ [$M = ReBr(CO)_3$ or $PtIme_3$]

(i) ^{13}C shifts for the carbonyl ligands in the complex $[ReBr(CO)_3(mcpt)]$ ^a

Major complex	Minor complex
190.33 (ax)	190.25 (ax)
193.37 (eq)	193.29 (eq)
197.07 (eq)	197.00 (eq)

(ii) 1H data for the methyl ligands in the complex $[PtIme_3(mcpt)]$ ^b

Major complex		Minor complex	
δ_H	$^2J_{PtH}/Hz$	δ_H	$^2J_{PtH}/Hz$
0.33 (eq)	70.0	0.39 (eq)	70.0
0.54 (ax)	72.0	0.51 (ax)	72.0
1.63 (eq)	74.0	1.66 (eq)	74.0

(iii) ^{195}Pt shifts for the complex $[PtIme_3(mcpt)]$ ^a

Major complex	Minor complex
1867.6 ^c	1871.2 ^c

^a In $(CDCl_2)_2$ at 303 K. ^b In $(CDCl_2)_2$ at 283 K. ^c Relative to $\Xi(^{195}Pt) = 21.4$ MHz.

estimate was made of the energy barrier for the rotation of the unsubstituted pyridyl ring of the major solution complex from the coalescence of the two low-temperature H_D signals (at δ 8.34 and 8.28). The ΔG^\ddagger value, calculated for the coalescence temperature of 203 K, was 42.2 kJ mol⁻¹. The population ratio of the two rotamers was 53%:47% at $-80^\circ C$. A similar study of the rotation of the 4-methylpyridine ring in the minor solution complex was carried out using the changes in the H_K signal. This split on cooling to low temperature into two signals (δ 9.03, 8.99) of approximately equal intensity. The coalescence temperature was again 203 K and ΔG^\ddagger (203 K) was estimated to be 43.2 kJ mol⁻¹. This slightly higher value to that of the unsubstituted pyridyl ring rotation in the major species could be the result of the steric effect of the methyl substituent.

Restricted rotation of the pendant rings was also evident in the complex $[PtIme_3(mcpt)]$. Cooling a CD_2Cl_2 solution to ca. $-80^\circ C$ caused a splitting of the ring methyl signals of both complex species. Rotamer populations, however, were now very different, relative populations being 86%:14% for pyridyl rotation in the major complex species and 89%:11% for 4-methylpyridyl rotation in the minor species. These rotamer populations are comparable to those found for $[PtIme_3(terpy)]$ (viz. 86.7:13.3%).² As in the previous work² the major rotamer species of $[PtIme_3(mcpt)]$ is attributed to that in which the pyridyl N atom is *cis* to the halogen analogous to that found in the crystal structure of $[PtIme_3(terpy)]$.²

Above-ambient temperature NMR studies

The main thrust of this work was to measure the dynamics of the fluxional shifts occurring in these complexes in solution, and to provide strong supporting evidence for the mechanism of the process.

All seven complexes (Table 1) showed evidence for this pro-

cess in their solution NMR spectra, but the rates, and temperature ranges over which spectral changes were detected, varied greatly according to the nature of the metal centre. In the unsymmetrical ligand complexes of mcpt, mmtt and bmtt, the fluxion causes interchange between the two different coordination complexes and leads to the following exchanges of ring hydrogens, $H_A \rightleftharpoons H_U$, $H_B \rightleftharpoons H_T$, $H_D \rightleftharpoons H_R$, $H_E \rightleftharpoons H_Q$, $H_F \rightleftharpoons H_P$, $H_G \rightleftharpoons H_N$, $H_H \rightleftharpoons H_M$, $H_I \rightleftharpoons H_L$ and $H_J \rightleftharpoons H_K$. In the mcpt complexes there are also additional exchanges $Me_C \rightleftharpoons Me_S$, $H_o \rightleftharpoons H_o'$ and $H_m \rightleftharpoons H_m'$. In the mmtt complex $Me_C \rightleftharpoons Me_S$ also occurs, and in the bmtt complex $Bu^t_C \rightleftharpoons Bu^t_S$ occurs. In the symmetrical ligand complex $[ReBr(CO)_3(mcpmt)]$, the fluxion interconverts chemically identical species (see Table 8), the exchanges being $H_A \rightleftharpoons H_J$, $H_B \rightleftharpoons H_I$, $Me_C \rightleftharpoons Me_H$, $H_D \rightleftharpoons H_G$ and $H_E \rightleftharpoons H_F$.

In the rhenium(i) and palladium(ii) complexes these changes were detected over a temperature range, ambient to 393 K, whilst for the platinum(iv) complexes the range was slightly lower, 273–353 K. For the platinum(ii) complexes the temperature range was considerably higher, with dynamic broadening of signals in one-dimensional spectra being detected only towards the high temperature limit of the solvent $(CDCl_2)_2$, around 403 K. The spectra of the complexes will now be discussed in turn.

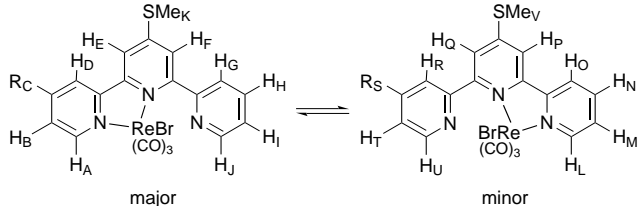
$[ReBr(CO)_3(mcpt)]$. The bandshapes of exchanging signals $Me_C \rightleftharpoons Me_S$ were fitted in the temperature range 303–393 K using the DNMR3 program,²³ and, in order to check for internal consistency, the ‘best-fit’ rate constants were used to simulate the exchanging ring hydrogen signals $H_A \rightleftharpoons H_U$ and $H_J \rightleftharpoons H_K$. Good agreement was found between experimental and computer simulated lineshapes, as seen in Fig. 3, when allowance was made for the temperature dependencies of the chemical shifts, and the scalar spin–spin couplings J_{AB} , J_{UT} , J_{KL} , J_{KM} , J_{JI} and J_{JH} were included. From these rate constants, reliable activation energies were obtained using the Eyring equation (Table 9).

$[ReBr(CO)_3L]$ ($L = mmtt, bmtt$). In these cases the fluxion was monitored by the signals of the exchanging pairs $H_A \rightleftharpoons H_U$ and $H_J \rightleftharpoons H_L$ in the temperature range 313–413 K. Bandshape analysis led to the activation energy data in Table 9.

$[ReBr(CO)_3(mcpmt)]$. For this complex, bandshape analysis was applied to the exchanging methyl signals $Me_C \rightleftharpoons Me_H$ using the DNMR3 program.²³

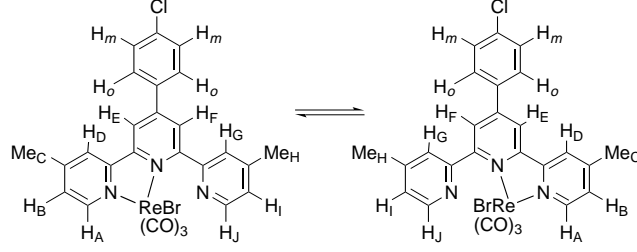
$[PtIme_3(mcpt)]$. Computer simulation was applied to the exchanging ring-methyl signals $Me_C \rightleftharpoons Me_S$ of this complex in the temperature range 273–343 K.

$[Pd(C_6F_5)_2(mcpt)]$. The methyl signals Me_C and Me_S were also studied in this case, in the temperature range 323–393 K. Good computer fits were again achieved and activation energy data calculated.

Table 7 Hydrogen-1 NMR data^a for the complexes [ReBr(CO)₃L] (L = mmtt or bmtt)


L	δ										
mmtt ^b	8.87 (A)	7.35 (B)	2.61 (C)	8.03 (D)	7.99 (E)	7.43 (F)	7.77 (G)	7.95 (H)	7.55 (I)	8.81 (J)	2.67 (K)
	8.65 (U)	7.35 (T)	2.51 (S)	7.61 (R)	7.47 (Q)	7.99 (P)	8.25 (O)	8.10 (N)	7.55 (M)	9.06 (L)	2.67 (V)
bmtt ^c	8.94 (A)	7.52 (B)	1.44 (C)	8.10 (D)	8.02 (E)	7.45 (F)	7.79 (G)	7.96 (H)	7.56 (I)	8.82 (J)	2.67 (K)
	8.70 (U)	7.52 (T)	1.39 (S)	7.72 (R)	7.45 (Q)	7.99 (P)	8.11 (O)	8.25 (N)	7.55 (M)	9.07 (L)	2.67 (V)

^a Chemical shifts recorded in (CDCl₂)₂ at 273 K, relative to internal SiMe₄ ($\delta = 0$). ^b R_C, R_S = Me. ^c R_C, R_S = Bu^t.

Table 8 Hydrogen-1 NMR data^a for the complex [ReBr(CO)₃(mcpt)]


δ											
8.89 (A)	7.35 (B)	2.61 (C)	8.32 (D)	8.11 (E)	7.88 (F)	7.64 (G)	2.52 (H)	7.35 (I)	8.64 (J)	7.72 (o)	7.54 (m)

^a Chemical shifts recorded in (CDCl₂)₂ at 283 K, relative to internal SiMe₄ ($\delta = 0$).

The fluxional process was also detected in the ¹⁹F spectra of the C₆F₅ ring fluorines. A detailed study of these changes, particularly using ¹⁹F 2-D-EXSY spectra, provided insight into the mechanism of the fluxion. However, discussion of these ¹⁹F spectra will be deferred until the spectra of [Pt(C₆F₅)₂(mcpt)] have been discussed below.

[Pt(C₆F₅)₂(mcpt)]. The ¹H NMR spectra of this complex recorded between room temperature and 413 K were essentially unchanged, indicating that any fluxion is slow on the ¹H NMR chemical shift timescale. The spectra at 413 K [the high-temperature limit of the (CDCl₂)₂ solvent] showed very slight line broadening in some of its signals. In order to confirm that the fluxion was occurring, albeit at a very slow rate, a ¹H 2-D-EXSY spectrum was recorded at 393 K with a mixing time of 0.8 s (Fig. 4). This showed clear cross-peaks associated with the exchanges H_B ⇌ H_T, H_L ⇌ H_I, H_H ⇌ H_M and H_J ⇌ H_K indicating the fluxional process. The D2DNMR program²⁴ was applied to this spectrum and a rate constant of 0.34 s⁻¹ was computed. This corresponds to a ΔG^\ddagger value of 100.6 kJ mol⁻¹ for the process at 393 K (Table 9).

Activation energies and mechanism of the fluxion

Activation energy data for the 1,4-M-N fluxions for the seven complexes are listed in Table 9. Values for the mcpt, mmtt and bmtt complexes relate to exchanges from major to minor solution complexes. The ΔG^\ddagger value for [Pt(C₆F₅)₂(mcpt)] is based on a single temperature and so is rather less accurate. The entropy changes, ΔS^\ddagger , range in magnitude from -22 to 22 J K⁻¹ mol⁻¹, but these values are not considered to provide any real insight into the nature of the fluxional process as they are extremely sensitive to systematic errors associated with the bandshape analysis process.

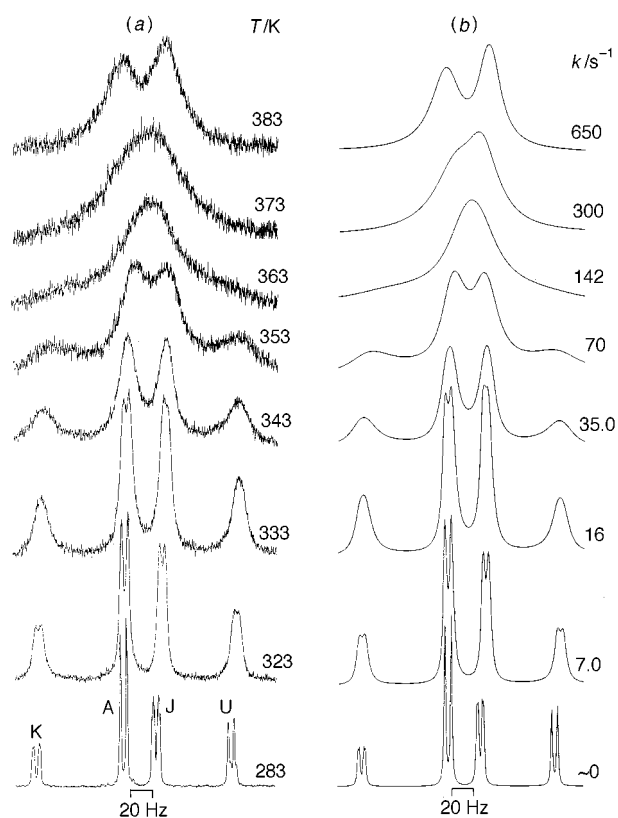


Fig. 3 Experimental (a) and computer simulated (b) spectra of the exchanging signals H_A ⇌ H_U and H_J ⇌ H_K in the complex [ReBr(CO)₃(mcpt)]. 'Best-fit' rate constants are given for each temperature

Table 9 Activation energy data^a for the 1,4 M–N fluxions in the complexes *fac*-[ReBr(CO)₃L] (L = mcpt, mcpmt, mmtt or bmtt) and [M(mcpt)] [M = Pt^{II}Me₃, Pt(C₆F₅)₂ or Pd(C₆F₅)₂]

Complex	Populations ^b (%)	$\Delta H^\ddagger/\text{kJ mol}^{-1}$	$\Delta S^\ddagger/\text{J K}^{-1} \text{mol}^{-1}$	$\Delta G^\ddagger (298 \text{ K})/\text{kJ mol}^{-1}$
[ReBr(CO) ₃ (mcpt)]	66:34	74.1 ± 2.6	−0.3 ± 0.1	74.1 ± 0.9
[Pt ^{II} Me ₃ (mcpt)]	63:37	72.8 ± 0.6	22.9 ± 1.9	66.0 ± 0.01
[Pt(C ₆ F ₅) ₂ (mcpt)]	64.5:35.5	—	—	100.6 ^c
[Pd(C ₆ F ₅) ₂ (mcpt)]	60:40	81.0 ± 1.0	21.1 ± 2.9	74.8 ± 0.2
[ReBr(CO) ₃ (mcpmt)]	50:50	72.5 ± 2.7	−0.4 ± 8.0	72.6 ± 0.4
[ReBr(CO) ₃ (mmtt)]	66:34	67.9 ± 1.8	−21.9 ± 4.9	74.4 ± 0.3
[ReBr(CO) ₃ (bmtt)]	61:39	69.5 ± 1.1	−17.7 ± 3.2	74.8 ± 0.2

^a For major → minor species (does not apply to mcpmt complexes). ^b Values ± 0.5%. ^c Calculated at 393 K from ¹H 2-D-EXSY spectrum (mixing time 0.8 s) with rate constant *k* of 0.344 s^{−1}.

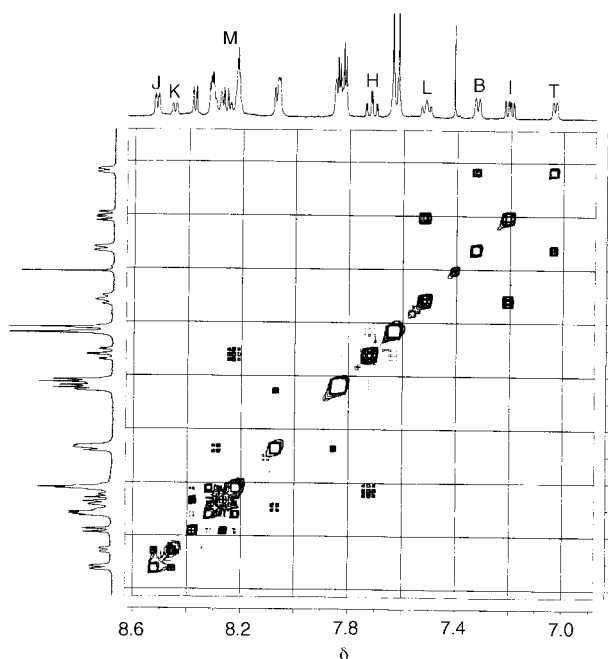


Fig. 4 400 MHz ¹H 2-D-EXSY NMR spectrum of [Pt(C₆F₅)₂(mcpt)] at 393 K in (CDCl₂)₂ showing slow fluxional exchange cross-peaks. Mixing time = 800 ms

The activation energies, $\Delta G^\ddagger (298 \text{ K})$, are more meaningful. Values vary in the range 66–101 kJ mol^{−1} and follow the trend Pt^{II} ≫ Pd^{II} ≈ Re^I > Pt^{IV}. For the rhenium(i) complexes there does not appear to be any clear dependence of ΔG^\ddagger on the nature of the ligand. For the metals Re^I and Pd^{II}, the ΔG^\ddagger values for the fluxion are slightly higher (by 1–4 kJ mol^{−1}) than for the corresponding terpy complexes.^{3,5} The approximate value of ΔG^\ddagger for the platinum(ii)–mcpt complex is *ca.* 6 kJ mol^{−1} higher than for the terpy complex analogue,⁵ whereas the value for the platinum(iv) complex [Pt^{IV}Me₃(mcpt)], is *lower*, by 7.9 kJ mol^{−1}, than the value of [Pt^{II}Me₃(terpy)].² The reason for this different trend is unclear.

We now turn to the question of the mechanism of these 1,4-M–N shifts. In our earlier work on the terpy complexes^{1–5} we discussed two possible mechanisms for the process, a rotation mechanism (i) and a tick-tock twist mechanism (ii), Fig. 5. The former involves a breaking of the M–N bond to the outer pyridyl ring followed by 180° rotation of the metal moiety and the metal then bonding to the third pyridyl ring. The M–N bond to the central pyridine ring remains intact, and the process causes no exchange of the groups attached to the metal *trans* to the M–N bonds. The twist mechanism (ii) involves a loosening of both M–N bonds followed by a twist of the metal moiety through an angle equal to the N–M–N angle of the original chelate ring. This process does lead to an exchange of the metal-attached groups *trans* to the M–N bonds. Evidence for the simultaneous occurrence of both mechanisms has been

obtained for ReX(CO)₃ and PtXMe₃ complexes of the chiral ligand 2,6-bis[4-(*S*)-methyloxazolin-2-yl]pyridine.²⁸ For the transition metal–terpy complexes the ‘tick-tock’ twist mechanism was favoured since the fluxion is accompanied by exchange of the spectator groups attached to the metal *trans* to the M–N bonds, namely the equatorial Pt–methyls in [PtXMe₃(terpy)] complexes, equatorial carbonyls in [ReX(CO)₃(terpy)] and C₆F₅ rings in [M(C₆F₅)₂(terpy)] (M = Pd^{II}, Pt^{II}) complexes.

However, these mechanisms (i) and (ii) have been questioned,⁸ and, in the case of the square-planar complexes [M(C₆F₅)₂(terpy)] (M = Pd^{II}, Pt^{II}), an isomerisation process (iii) based on a T-shaped, 14-electron, three-co-ordinate intermediate proposed (Fig. 5).

The fluxionality of the mcpt complexes of Pt^{II} and Pd^{II} interconverts chemically distinct species and allows the mechanism of the fluxion to be monitored unambiguously by its effect on the spectator groups (*viz.* C₆F₅ rings) attached to the metal in the *trans*-N positions. The rotation process [mechanism (i)] would cause the C₆F₅-rings to exchange in the manner A ⇌ D and B ⇌ C (see Table 4), the associative tick-tock twist process [mechanism (ii)] would lead to the pair-wise exchanges A ⇌ C and B ⇌ D, whereas the isomerisation process [mechanism (iii)] would lead to exchange of all four signals. A ¹⁹F NMR study of [Pt(C₆F₅)₂(mcpt)] proved to be most definitive. A ¹⁹F 2-D-EXSY spectrum of the *para*-F signals of this compound at 413 K in (CDCl₂)₂ solvent (Fig. 6) showed clear cross-peaks for the two specific exchanges A ⇌ C and B ⇌ D, and no others. Very analogous results were obtained from the ¹⁹F 2-D-EXSY spectrum of the *ortho*-F signals of [Pd(C₆F₅)₂(mcpt)] at 323 K, and from the ¹H 2-D-EXSY spectrum of the equatorial Pt-methyl signals of [Pt^{II}Me₃(mcpt)] at 273 K. These double pair-wise exchanges between the M-bonded spectator ligands in these palladium(ii) and platinum(ii), -(iv) complexes provide definitive evidence for an associative ‘tick-tock’ twist movement of the metal moiety which proceeds *via* an intermediate having a quasi-terdentate ligand (Fig. 7). It was not possible to provide firm evidence that the associative process also occurs in the present rhenium(i) complexes because it was not possible to obtain a ¹³C 2-D-EXSY spectrum of the equatorial carbonyl signals. However, platinum(iv) and rhenium(i) terpy complexes have the same fluxional mechanisms^{2,3} and so it is assumed that the same applies here. A dissociative process, in the case of the square-planar palladium(ii) and platinum(ii) complexes, would probably involve a three-co-ordinate T-shaped intermediate of the type proposed by Minniti¹⁴ and Romeo *et al.*²⁹ in connection with the isomerisation of palladium(ii) and platinum(ii) complexes of sulfur-bonded ligands. In the case of the present octahedral complexes of Re^I and Pt^{IV}, being involved in a dissociative process the likely intermediate would be a five-co-ordinate trigonal-bipyramidal structure. Both these three- and five-co-ordinate intermediates would be expected to be highly fluxional, displaying rapid isomerisation and rotation about the M–N bond to the central pyridyl ring, leading to total exchange of all four equatorial spectator ligands. This clearly does *not*

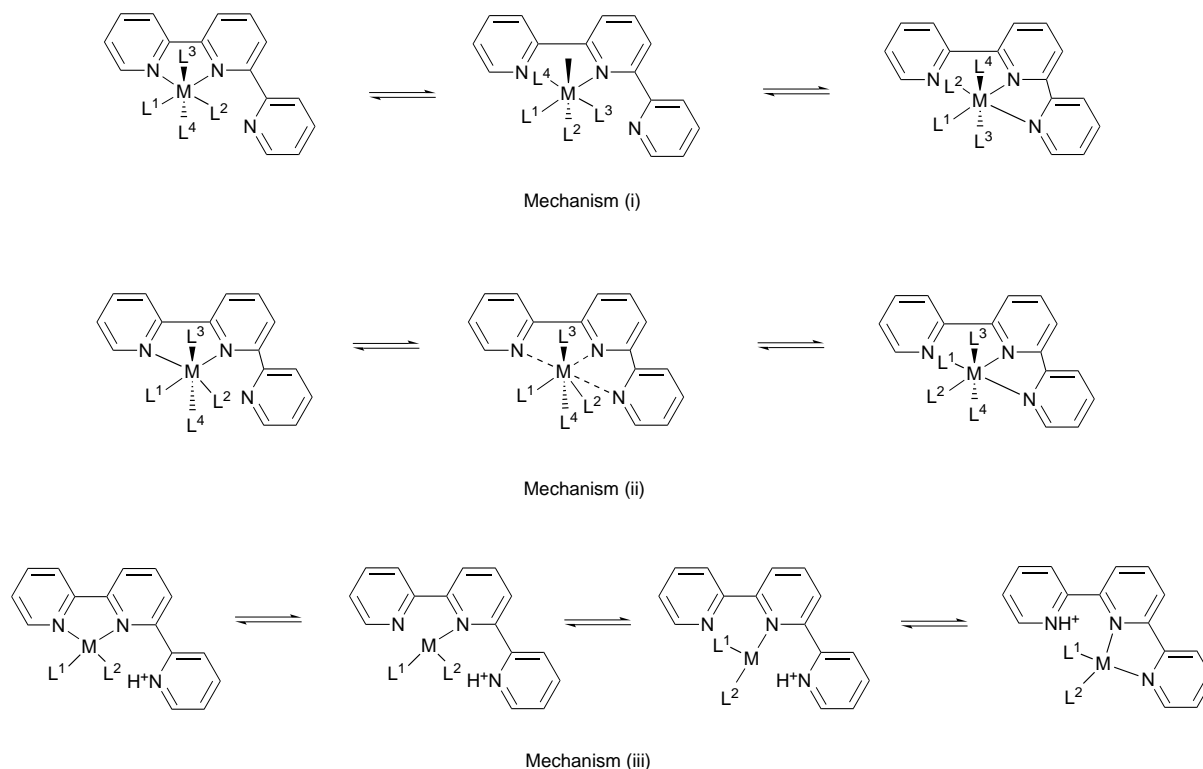


Fig. 5 Mechanisms of M–N linkage fluxion in metal chelate complexes, namely the rotation mechanism (i), the associative ‘tick-tock’ twist mechanism (ii) and the isomerisation mechanism (iii)

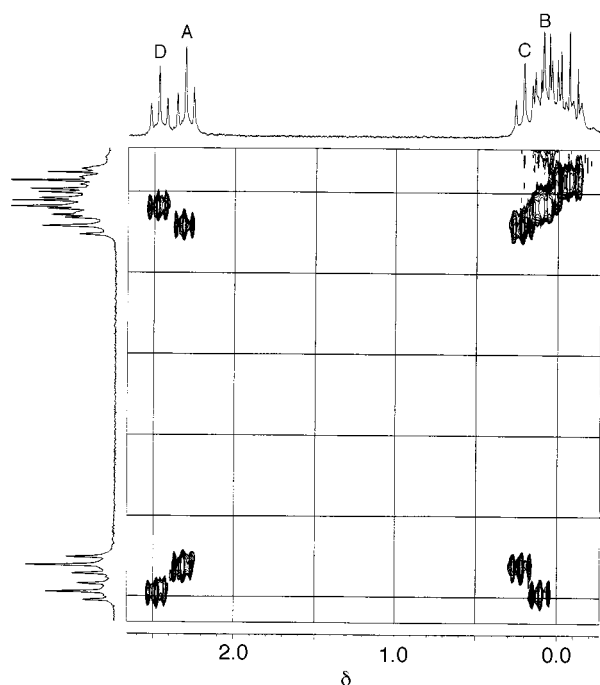


Fig. 6 ^{19}F 2-D-EXSY NMR spectrum of $[\text{Pt}(\text{C}_6\text{F}_5)_2(\text{mcpt})]$ in $(\text{CDCl}_2)_2$ at 413 K showing the *para* ring fluorine signals of the four C_6F_5 rings A–D. Cross-peaks define the two pair-wise exchanges $\text{A} \rightleftharpoons \text{C}$ and $\text{B} \rightleftharpoons \text{D}$ (see Table 4 for labelling). Triplet splittings are due to $^3J_{\text{FF}}$ couplings (ca. 19.3 Hz). Additional multiplet near δ 0 is due to some of the *meta* ring fluorines. Mixing time for the experiment was 800 ms

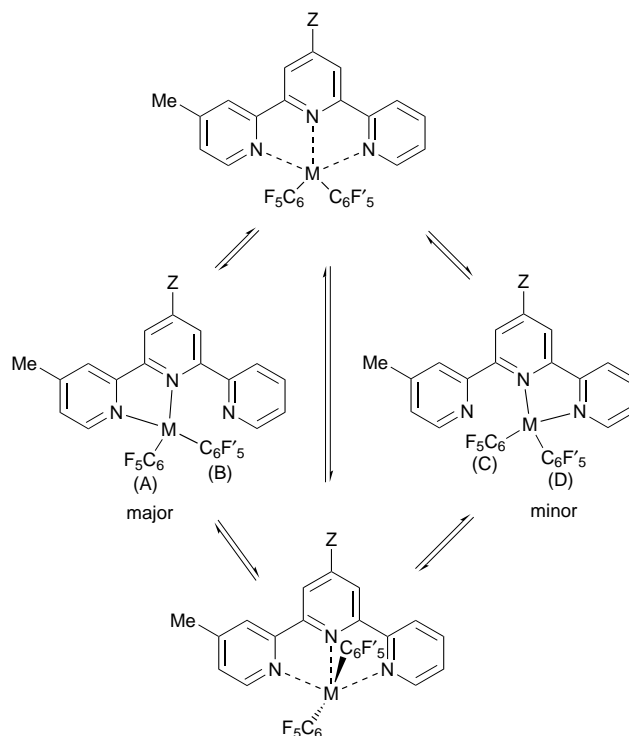


Fig. 7 The 1,4-metallotropic shift occurring *via* an associative mechanism in the complexes $\text{cis-}[\text{M}(\text{C}_6\text{F}_5)_2(\text{mcpt})]$ ($\text{Z} = 4\text{-chlorophenyl}$) showing the selective exchanges $\text{A} \rightleftharpoons \text{C}$ and $\text{B} \rightleftharpoons \text{D}$. Possible distortion towards a trigonal-bipyramidal geometry is shown, but this distortion must not lead to a loss of identity of the C_6F_5 and $\text{C}_6\text{F}_5'$ rings

occur. The process actually occurring may therefore be described as an associative, oscillatory, ‘tick-tock’ or windscreen-wiper motion of the metal moiety through an angle equal to the N–M–N angle at the metal centre.

The geometries and bonding of the proposed intermediates in these fluxional processes raise interesting theoretical speculation. In the square-planar palladium(II) or platinum(II) com-

plexes the intermediate would appear to be a planar quasi-five-coordinate structure (Fig. 7). Distortions from planarity, *e.g.* *via* Berry pseudo-rotations, towards trigonal-bipyramidal or square-pyramidal structures, may occur but they must be totally reversible, otherwise exchange of all equatorial spectator ligands will occur. Near-planar five-coordinate geometries are highly unusual and are worthy of theoretical investigation.

In the octahedral platinum(IV) and rhenium(I) complexes the likely intermediate would appear to be a seven-coordinate pentagonal bipyramid. Such a geometry is normally highly non-rigid. However, in the present platinum(IV) complexes of mcpt, the 'tick-tock' twist fluxion does not produce any exchange of equatorial and axial Pt–methyl environments {such Pt–methyl scrambling only occurs at higher temperatures in [Pt(Me)₃(mcpt)]}, so the seven-coordinate intermediate does appear to exhibit some considerable degree of stereochemical rigidity, a conclusion which again merits theoretical study.

Acknowledgements

We are grateful to Professor Eddie Abel for fruitful discussions. We thank the EPSRC for a postdoctoral research fellowship (to A. G.).

References

- 1 E. W. Abel, N. J. Long, K. G. Orrell, A. G. Osborne, H. M. Pain and V. Šik, *J. Chem. Soc., Chem. Commun.*, 1992, 303.
- 2 E. W. Abel, V. S. Dimitrov, N. J. Long, K. G. Orrell, A. G. Osborne, V. Šik, M. B. Hursthouse and M. A. Mazid, *J. Chem. Soc., Dalton Trans.*, 1993, 291.
- 3 E. W. Abel, V. S. Dimitrov, N. J. Long, K. G. Orrell, A. G. Osborne, H. M. Pain, V. Šik, M. B. Hursthouse and M. A. Mazid, *J. Chem. Soc., Dalton Trans.*, 1993, 597.
- 4 E. W. Abel, K. G. Orrell, A. G. Osborne, H. M. Pain and V. Šik, *J. Chem. Soc., Dalton Trans.*, 1994, 111.
- 5 E. W. Abel, K. G. Orrell, A. G. Osborne, H. M. Pain, V. Šik, M. B. Hursthouse and K. M. A. Malik, *J. Chem. Soc., Dalton Trans.*, 1994, 3441.
- 6 E. R. Civitello, P. S. Dragovich, T. B. Karpishin, S. G. Novick, G. Bierach, J. F. O'Connell and T. F. Westmoreland, *Inorg. Chem.*, 1993, **32**, 237.
- 7 S. Ramdeehul, L. Barloy, J. A. Osborn, A. de Cian and J. Fischer, *Organometallics*, 1996, **15**, 5442.
- 8 T. Daniel, N. Suzuki, K. Tanaka and A. Nakamura, *J. Organomet. Chem.*, 1995, **505**, 109.
- 9 E. Rotondo, G. Giordano and D. Minniti, *J. Chem. Soc., Dalton Trans.*, 1996, 253.
- 10 E. W. Abel, A. Gelling, K. G. Orrell, A. G. Osborne and V. Šik, *Chem. Commun.*, 1996, 2329.
- 11 (a) H. D. Kaesz, R. Bau, D. Hendrickson and J. M. Smith, *J. Am. Chem. Soc.*, 1967, **89**, 2844; (b) M. M. Bhatti, Ph.D. Thesis, University of Exeter, 1980.
- 12 D. H. Goldsworthy, Ph.D. Thesis, University of Exeter, 1980.
- 13 G. Lopez and G. Garcia, *Inorg. Chim. Acta*, 1981, **52**, 87; G. Lopez, G. Garcia, N. Cutillas and J. Ruiz, *J. Organomet. Chem.*, 1983, **241**, 269.
- 14 D. Minniti, *Inorg. Chem.*, 1994, **33**, 2631.
- 15 W. K. Fife, *J. Org. Chem.*, 1983, **48**, 1375.
- 16 F. H. Case and T. J. Kasper, *J. Am. Chem. Soc.*, 1956, **78**, 5842.
- 17 P. H. Ko, T. Y. Chen, J. Zhu, K. F. Cheng, S. M. Peng and C. M. Che, *J. Chem. Soc., Dalton Trans.*, 1995, 2215.
- 18 F. Krohnke and K. F. Gross, *Chem. Ber.*, 1959, **92**, 22.
- 19 F. Krohnke, *Synthesis*, 1976, 1.
- 20 E. C. Constable and A. M. W. Cargill-Thompson, *New J. Chem.*, 1996, **20**, 65 and refs. therein.
- 21 K. T. Potts, D. A. Usifer, A. Guadalupe and H. D. Abruna, *J. Am. Chem. Soc.*, 1987, **109**, 3961; K. T. Potts, P. Ralli, G. Theodoridis and P. Winslow, *Org. Synth.*, 1986, **64**, 189.
- 22 D. F. Shriver, *Manipulation of Air-Sensitive Compounds*, McGraw-Hill, New York, 1969.
- 23 D. A. Kleier and G. Binsch, DNMR3 Program 165, Quantum Chemistry Program Exchange, Indiana University, IN, 1970.
- 24 E. W. Abel, T. P. J. Coston, K. G. Orrell, V. Šik and D. Stephenson, *J. Magn. Reson.*, 1986, **70**, 34.
- 25 V. Šik, Ph.D. Thesis, University of Exeter, 1979.
- 26 C. A. Bessel, R. F. See, D. L. Jameson, M. R. Churchill and K. J. Takeuchi, *J. Chem. Soc., Dalton Trans.*, 1992, 3223.
- 27 E. W. Abel, K. A. Hylands, M. D. Olsen, K. G. Orrell, A. G. Osborne, V. Šik and G. N. Ward, *J. Chem. Soc., Dalton Trans.*, 1994, 1079.
- 28 P. J. Heard and C. Jones, *J. Chem. Soc., Dalton Trans.*, 1997, 1083.
- 29 R. Romeo, A. Grassi and L. Monsù Scolaro, *Inorg. Chem.*, 1992, **31**, 4383.

Received 18th November 1997; Paper 7/08293B